Proc. Natl. Acad. Sci. USA
Vol. 92, pp. 9796–9800, October 1995
Biochemistry

X-ray structure of clotting factor IXa: Active site and module structure related to Xase activity and hemophilia B

(x-ray crystallography/coagulation factors/serine proteinase/epidermal growth factor-like domains)

HANS BRANDSTETTER*, MARGIT BAUER*, ROBERT HUBER*, PETE LOLLAR†, AND WOLFRAM BODE*‡

*Max-Planck-Institut für Biochemie, D82152 Martinsried, Germany; and †Emory University School of Medicine, Department of Medicine, Woodruff Memorial Building, Atlanta, GA 30322

Contributed by Robert Huber, July 10, 1995

ABSTRACT **Hereditary deficiency of factor IXa (fIXa), a key enzyme in blood coagulation, causes hemophilia B, a severe X chromosome-linked bleeding disorder afflicting 1 in 30,000 males; clinical studies have identified nearly 500 deleterious variants. The x-ray structure of porcine fIXa described here shows the atomic origins of the disease, while the spatial distribution of mutation sites suggests a structural model for factor X activation by phospholipid-bound fIXa and cofactor VIIIa. The 3.0-Å-resolution diffraction data clearly show the structures of the serine proteinase module and the two preceding epidermal growth factor (EGF)-like modules; the N-terminal Gla module is partially disordered. The catalytic module, with covalent inhibitor D-Phe-1I–Pro-2I–Arg-3I chloromethyl ketone, most closely resembles fXa but differs significantly at several positions. Particularly noteworthy is the strained conformation of Glu-388, a residue strictly conserved in known fIXa sequences but conserved as Gly among other trypsin-like serine proteinases. Flexibility apparent in electron density together with modeling studies suggests that this may cause incomplete active site formation, even after zymogen activation, and hence the low catalytic activity of fIXa. The principal axes of the oblong EGF-like domains define an angle of 110°, stabilized by a strictly conserved and fIX-specific interdomain salt bridge. The disorder of the Gla module, whose hydrophobic helix is apparent in electron density, can be attributed to the absence of calcium in the crystals; we have modeled the Gla module in its calcium form by using prothrombin fragment 1. The arched module arrangement agrees with fluorescence energy transfer experiments. Most hemophilic mutation sites of surface fIX residues occur on the concave surface of the bent molecule and suggest a plausible model for the membrane-bound ternary fIXa–fVIIIa–fX complex structure: fIXa and an equivalently arranged fX arch across an underlying fVIIIa subdomain from opposite sides; the stabilizing fVIIIa interactions force the catalytic modules together, completing fIXa active site formation and catalytic enhancement.**

Human factor IX (fIX) is secreted as a 415-residue single-chain molecule into the blood, where it is activated to fIXa by proteolytic cleavage (1–3). A single cleavage at Arg-180–Val-181 [Arg-181–Ile-182 in porcine fIX (refs. 4–6; P.L., unpublished data)], corresponding to residues 15 and 16 in chymotrypsinogen numbering (hereafter denoted with the prefix c) generates active form fIXaα, while a second cleavage removes segment Ala-146–Arg-180 to generate the physiological active form fIXaβ (7, 8). The N-terminal light chain (145 residues) and the C-terminal heavy chain (235 residues) are disulfide linked via Cys-132–Cys-289(c122). The light chain consists of several modules, which also reflect the exon structure (9): the N-terminal Gla module (residues 1–38; Gla refers to C^{γ} carboxylated glutamic acid residues) followed by its hydrophobic helix (39–46), two epidermal growth factor (EGF)-like domains (residues 47–84 and 85–127), and a linker peptide (residues 128–145); the heavy chain (residues 181–415) forms the catalytic module. Free fIXaβ is an extremely poor proteinase (10–14) but becomes a potent fX activator upon complex formation with its cofactor fVIIIa via calcium-mediated binding *in vitro* to anionic phospholipid membranes and *in vivo* to the surfaces of endothelial cells or activated platelets (15). This complex, Xase of the intrinsic blood coagulation pathway, converts fX to fXa by cleavage of the Arg-194–Ile-195(c16) peptide bond.

X-ray structures are available for the coagulation factors thrombin and several thrombin complexes (16–19), of prothrombin fragment 1 [consisting of a Gla domain and kringle 1 (20, 21)], and of fXa, in which the EGF-1 module is disordered and the Gla domain is absent (22). In addition, NMR structures have been reported for the EGF-1 and EGF-2 domains of fIX and fX (23, 24) and for the calcium-free Gla–EGF-1 domain pair of bovine fX and calcium-free Gla domain of fIX Gla (25, 26). The structure of fIXaβ, a full-length, membrane-dependent coagulation factor, is presented here.§

MATERIALS AND METHODS

Porcine fIXaβ was prepared and blocked with D-Phe-1I–Pro-2I–Arg-3I chloromethyl ketone (PPACK) as described (27, 28). PPACK–fIXaβ was crystallized by vapor diffusion at room temperature in 22% PEG 6000 and 0.5 M sodium acetate (pH 6.6). The crystals of tetragonal space group $P4_12_12$ have cell constants $a = b = 128.75$ Å, $c = 77.00$ Å, with one molecule per asymmetric unit. Native data to 3 Å resolution were collected on a MAR image plate at 4°C. Due to partial anisomorphism, only 37,000 reflections from the best native crystal were evaluated with MOSFLM, Version 5.1 (A. G. W. Leslie, Mosflm User Guide, Cambridge, U.K.), and merged with CCP4 routines (29) yielding 12,050 independent reflections (89.2% completeness). Orientation and position of the catalytic domain were determined with X-PLOR routines (30), using trypsin and fXa (22) polyalanine models. The catalytic domain was improved and refined against 3-Å electron density maps using MAIN (31) and X-PLOR routines. The final density allowed localization of the EGF-2/linker module. Eventually the EGF-1 domain was localized using AMORE (32). Cylindrical electron density beyond the N-terminal pole of EGF-1 could account for the C-terminal helix of the Gla domain. This

The publication costs of this article were defrayed in part by page charge payment. This article must therefore be hereby marked "*advertisement*" in accordance with 18 U.S.C. §1734 solely to indicate this fact.

Abbreviations: fIX, factor IX; EGF, epidermal growth factor; PPACK, D-Phe-1I–Pro-2I–Arg-3I chloromethyl ketone.

‡To whom reprint requests should be addressed.

§The atomic coordinates and structure factors have been deposited in the Protein Data Bank, Chemistry Department, Brookhaven National Laboratory, Upton, NY 11973 (reference 1PFX). This information is embargoed for 1 year (coordinates) and 5 years (structure factors) from the date of publication.

feature has allowed us to model the Gla domain of fIXaβ in the presence of calcium by positioning the hydrophobic stack of calcium-bound prothrombin fragment 1 (21) in this density. Since crystals are not destroyed by calcium soaking experiments, the Gla domain position should also be compatible with crystal packing (see Fig. 1). This full-length model was crystallographically refined to an R value of 0.198, including 10,693 reflections from 8.0 to 3.0 Å. The rms deviations of this model from standard bond lengths and angles are 0.010 Å and 2.01°.

RESULTS AND DISCUSSION

The structure of fIXaβ resembles a tulip, with the catalytic module representing the flower, the two interlaced EGF domains the bent stalk, and the N-terminal Gla domain the bulb (Fig. 1). The lengths including the bend and the maximal spatial extension of the molecule are 130 and 105 Å, respectively. The catalytic module possesses the typical fold of trypsin-like serine proteinases and closely resembles that of fXa. The ammonium group of N-terminal Ile-181(c16) forms a buried salt bridge with Asp-364(c194), characteristic for an "active" serine proteinase, in agreement with the unfavorable effect of mutations of either fIX residue on coagulation activity (35).

In its active site groove the PPACK inhibitor is covalently linked to the catalytic residues Ser-365(c195) and His-221(c57) (Fig. 2), similar to PPACK thrombin (16, 17). Its peptidic chain forms twisted antiparallel β-sheet hydrogen bonds with fIXa residues Ser-384(c214)–Gly-386(c216). The S1 specificity pocket accommodates the extended Arg-3I side chain, which forms a salt bridge with the Asp-359(c189) carboxylate group at its bottom. Hemophilia B associated with mutations in and around this pocket can be attributed to impaired S1 formation or defective substrate recognition (36–38, 62).

Tyr-266(c99) is displaced compared to its position in fXa (22), occupying the aromatic site formed in fXa by Tyr-266(c99), Trp-385(c215), and Phe-342(c174). As a result, the S2 site of fIXaβ is more open, accommodating Pro-2I as well as Thr, Val, Phe, or Trp P2 residues found in natural or synthetic substrates (10–15); the benzyl group of D-Phe-1I is not buried (Fig. 2).

The frame to the entrance of the fIXaβ specificity pocket, segment Ser-384(c214)–Cys-389(c220), conforms to the typical conformation of other trypsin-like serine proteinases (Fig. 2); however, the sequence Gly-386(c216)–Glu-387(c217)–Glu-388(c219)–Cys-389(c220) shows greater mobility. In particular Glu-388(c219), whose carbonyl points toward NH_2 of Arg-3I, is only weakly defined and exhibits a high-energy main-chain conformation ($\Phi = 55°$, $\Psi = -164°$), usually confined to Gly residues. This may cause its greater flexibility relative to the other trypsin-like enzymes, which all have Gly at this position; Glu-388(c219) is strictly conserved in the seven fIX sequences determined so far (4–6). The quality of the electron density is sufficient to reliably establish structural mobility, since at adjoining sites Phe-342(c174) and Gln-362(c192) the density correctly predicted sequence corrections (S. S. Sommer, personal communication) of Val → Phe and Ile → Gln from the published cDNA sequencing (5). Molecular dynamics simulations, using model coordinates after elimination of PPACK, indicate a destabilization of Glu-388(c219) including its carbonyl group. This leads to a partial collapse of the pocket incompatible with normal substrate binding; such destabilization is not evident in equivalent molecular dynamics simulations of fXa with its typical Gly at 388(c219).

Such an incompletely formed specificity pocket might explain the reduction in catalytic efficiency (k_{cat}/K_m) of fIXaβ by several orders of magnitude toward chromogenic amide substrates compared with fXa (10–14). Hindered recognition and binding of basic peptidic substrates and chloromethyl ketone inhibitors would correspond to unproductive approaches of the scissile peptide bond or reactive groups, respectively. For

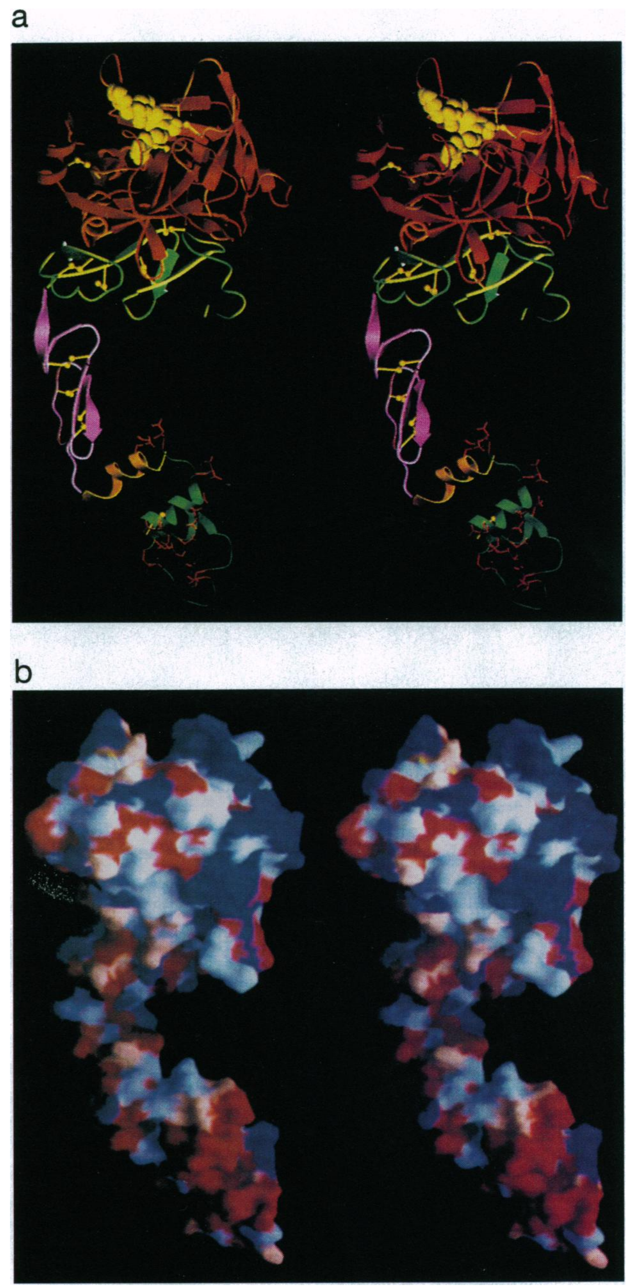

FIG. 1. Ribbon plot [*a*; SETOR (33)] and solid surface model [*b*; GRASP (34)] of the bent fIXaβ molecule. The phospholipid membrane is presumed to bind to the Gla domain (bottom) approximately along a horizontal plane. PPACK (yellow) is bound to the active site of the catalytic domain (top). (*a*) Light chain consists of the N-terminal Gla domain/hydrophobic stack model (green/yellow) with the Gla residues (red ball and stick) shown explicitly, followed by EGF-1 (magenta) and EGF-2/linker peptide (light green); heavy chain forms the catalytic domain (red). (*b*) Surface is colored according to residue conservation; mutations that lead to bleeding disorders are red, fIX-specific conserved residues are pink, other conserved fIX residues are light blue, and variable residues are blue. Concave side facing the front and the strip to the left of the molecule are dominated by hemophilic mutations, fIX-specific or conserved residues and are therefore implicated in fVIIIa binding while right and back sides display more variable residues.

example, benzamidine binding would require rigidification of the 388(c219) carbonyl group into the S1 pocket-forming position, with an energy cost reflected in the 15- and 100-fold lower affinity (larger K_i) for fIXaβ compared to fXa and thrombin (P.L., unpublished data). This destabilized state of fIXaβ is reminiscent of the mobile and occluded S1 pocket of

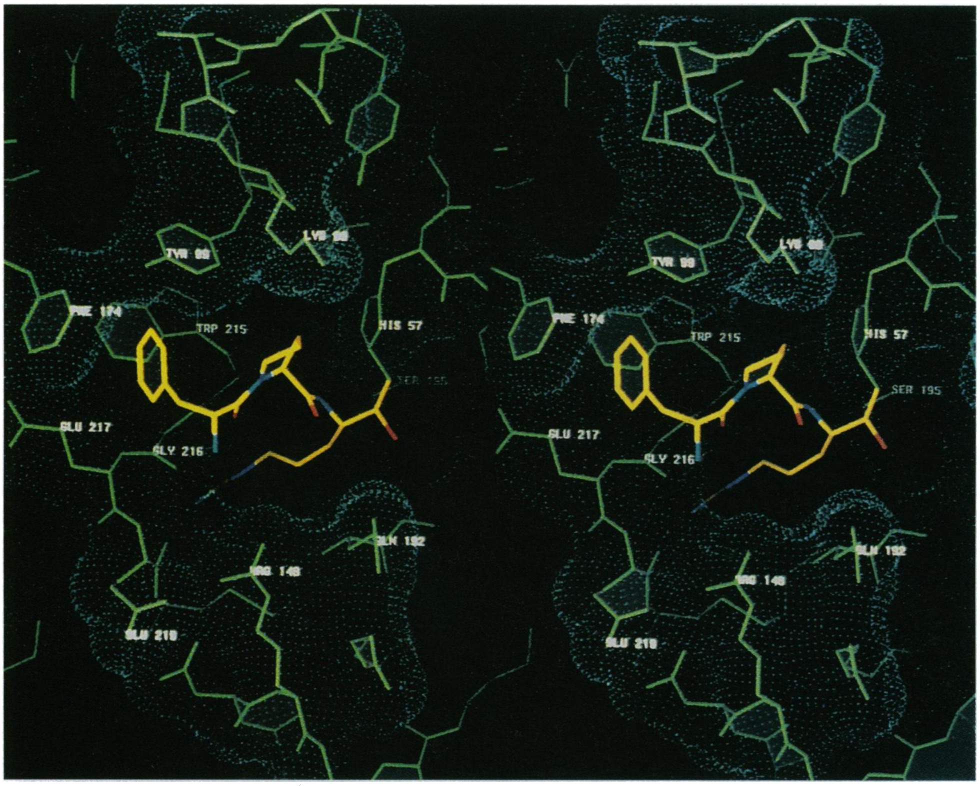

FIG. 2. PPACK (yellow) bound to the active site region of fIXaβ (green) superimposed with a Connolly dot surface [MAIN (31)] related to the view in Fig. 1 by a 90° rotation about a horizontal axis in the plane of the page. Specificity pocket opens to the left of the active site residues (right), with its entrance framed by the kinked segment Trp-385(c215)–Cys-389(c220). Due to the high-energy conformation of Glu-388(c219) (bottom left), this frame is mobile and would presumably collapse upon removal of the inhibitor.

the trypsinogen-like zymogens, which generally precludes binding of substrates and inhibitors but can be forced into the active state by very high-affinity active site binding (39–43).

The linker peptide of fIXaβ sits in a depression on a pole of the catalytic module surface opposite the active site residues. This peptide forms a disulfide to the catalytic domain with Cys-132–Cys-289(c122) and is defined to His-139. In the N-terminal direction, it links the catalytic module with the EGF-2 domain, which also associate through a common aromatic-rich interface, similar to fXa (22). Both EGF-like domains of fIXaβ are similar to the EGF-2 domain of human fXa and the isolated EGF-1 domains of human and bovine fIXa (22–24). They resemble an axe head, with five consecutive peptide strands linked in pairs through four β-hairpin loops and cross-connected via three disulfide bridges (see Fig. 1*a*). Strand 1 is rather kinked, while pairs of strands 2–3 and 4–5 form a "major" and a "minor" twisted β-pleated sheet, respectively.

The domain structure of fIXa provides important clues to structural aspects of its function in Xase. The head-to-tail arrangement of both EGF domains, which are also related by a rough 180° screw axis along their long axes, which in turn define an angle of 110°, is probably important for fIXa function. The interdomain interface comprises ≈80 atomic contacts below 4.0 Å and resembles a ball-and-socket joint (Fig. 1*a*), where EGF-1 would revolve about its exposed and hydrophobic s3 → s4 loop (Val-75–Gly-76–Phe-77), set in a concave EGF-2 hydrophobic socket formed by the strictly conserved residues Val-107, Cys-109, Ala-86, and the hydrophobic side chain parts of Lys-122 and Arg-94. "Joint" rotation is restricted, however, by three additional contacts, provided by (*i*) the (covalent) connecting segment Glu-83–Leu-84–Asp-85–Val-86, (*ii*) a polar hydrogen bond formed between the conserved basic group of Lys-122 and Gln-74 O, and especially (*iii*) a salt bridge between Glu-78 and Arg-94 (Fig. 3), both strictly conserved among fIX sequences. The conservation and extent of these interactions argues that the relative spatial orientation described here is an intrinsic structural property of fIXa relatively unaffected by crystal packing.

A calcium binding site has been located (23, 24) at the N-terminal pole of the EGF-1 domain between the entering strand 1 and the s2 → s3 hairpin loop (Asp-64–Ser-68). Three of the calcium ligands—Asp-65, Gln-50, and Asp-64—are suitably oriented for calcium binding in the fIXaβ structure. Due to lack of calcium, however, this site is not occupied, presumably causing some disorder in the EGF-1 connecting segment from Asp-47 to Gln-50 (24).

Several lines of evidence (20, 21, 44–48) suggest that in the absence of calcium the interaction between EGF-1 and the C-terminal helix of the Gla domain (i.e., the hydrophobic stack) is weak; the helical topology of the Gla domain conforms to the calcium-bound Gla domain on average, albeit with higher mobility of the secondary structure elements (25, 26). The crystal structure of prothrombin fragment 1 determined in the absence of calcium placed the α-helical hydrophobic stack adjacent to the kringle 1 domain (20); calcium binding induces a conformational transition to a more ordered structure, with several Gla residues becoming partially buried and membrane binding determinants such as Leu-6 or Phe-9 exposed (21, 25, 26).

According to this model, the EGF-1 domain of fIXaβ interacts with the Gla domain mainly through the strictly conserved Ile-66 and the preceding s2 → s3 loop of EGF-1 and the side chains of Asn-39 and Lys-43 of the hydrophobic stack. Gla-36 and Gla-40, 2 of the 12 fIXa Gla residues not present in prothrombin, point toward the EGF-1 domain, the latter possibly making a salt bridge to the strictly conserved Lys-63. As in prothrombin (21), the first 9 Gla residues together with the exposed hydrophobic residues of the Ω-loop (Fig. 1*a*) are most likely responsible for calcium-dependent phospholipid membrane binding in a not fully understood manner (21, 25, 26, 44–48). The 90-Å distance between the D-Phe-1I of fIXaβ bound PPACK and the center of the Ω-loop is consistent with distances of 89 and 73 Å between D-Phe-1I-conjugated fluorescence donors and membrane-bound acceptor dyes obtained from fluorescence energy transfer measurements (49) if a horizontal membrane orientation is assumed as in Fig. 1.

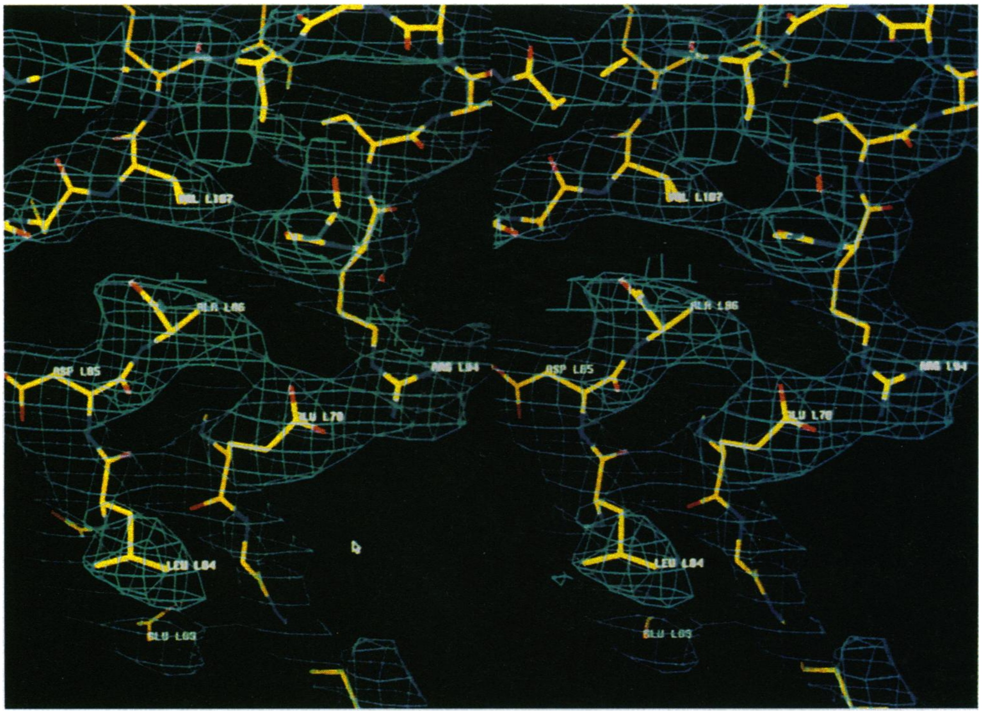

FIG. 3. Thin section of the final electron density map through the EGF-1–EGF-2 interface of fIXaβ. The unique salt bridge, formed between the fIX-specific conserved residues Glu-78 (EGF-1) and Arg-94 (EGF-2) (right), and part of the connecting segment Leu-84–Asp-85–Ala-86 (left) are shown.

Another important aspect is the interaction of fIXa with cofactor VIIIa and substrate fX. Competition experiments with various enzyme fragments and chimeric molecules suggest that both the light and heavy chains of fIXa bind to fVIIIa, with somewhat weaker participation of the EGF-1 domain (50–54). Residues particularly important to the fIXa–fVIIIa interaction should be highly conserved, at the molecular surface, specific to the coagulation factor (fIXa or fVIIIa), and sensitive to mutation (and hence observable either through clinical recognition of naturally occurring hemophilic variants of high antigenic level or through clinical recognition of naturally occurring hemophilic variants of high antigenic level or through site-directed mutagenesis experiments). Examination of the fIXaβ surface according to these criteria reveals a continuous broad strip, a kind of hemophilic surface, extending along the entire concave surface of the fIXa molecule (Fig. 1*b*), partially enclosing a hollow, which probably represents the binding site of fVIIIa.

Specific residues associated with hemophilic mutations that contribute to this putative fVIIIa binding surface can be found in each domain of the light chain: in the Gla domain, Phe-9 (in the Ω-loop) and Phe-25 and Arg-29 (in the second helix) are exposed and point toward the hollow created by the arched fIXaβ modules; each is strictly conserved in fIX. Ile-66, Tyr-69, and Trp-72 (55) of the EGF-1 domain likewise face the hollow; the latter is remarkably exposed and specifically conserved in fIX. The same holds true for the side chains of the strictly conserved EGF-2 residues Ile-90, Asn-92, and Arg-94 (the latter involved in the fIX-specific salt bridge with Glu-78).

In contrast, O-glycosylation of Ser-53 and Ser-61 of EGF-1 (56) in several fIX species (4–6) indicates that the convex surface opposite the hollow is not involved in fVIIIa binding. In general, this surface of the light chain (not visible in Fig. 1) is less conserved and lacks sites of hemophilic mutations.

The α-helix Leu-330(c162)–Arg-338(c170) of the catalytic module of fIXaβ is a site of particularly numerous mutations (red patch on the upper left of Fig. 1*b*). Mutations in 6 of the 9 highly conserved residues manifest themselves in bleeding disorders (cf. refs. 36–38). Arg-333(c165) forms part of a contiguous positively charged surface patch, which is a potential anchoring site for acidic glycosaminoglycans such as heparin. Heparin binds more tightly to fIXaβ and to fX or fVIIIa but inhibits the activity of intrinsic Xase noncompetitively rather than impairing assembly (57).

In the fIX zymogen, the 35-residue activation peptide is presumably located on the front surface in Fig. 1. The zymogen fIX is known not to form a complex with fVIIIa (51–53). Cleavage of the zymogen only at Arg-180(c15)–Ile-181(c16) results in the active species fIXaα; full cofactor binding activity requires additional cleavage at Arg-145–Ala-146 and removal of the activation peptide (2), suggesting sterical hindrance by the peptide. fIXa cleavage of fX also requires conservation of residues in the vicinity of the active site, in agreement with observed mutations of conserved surface residues resulting in hemophilia B (36–38).

In the absence of a suitable phospholipid membrane surface and of fVIIIa, collisional encounters leading to binding of fIXaβ and fX occur rarely, reflected in the very large K_m value of 33,000 nM; in addition, the catalytic efficiency is low, with a k_{cat} of 0.003 sec^{-1} (57–59). Binding to phospholipid membrane restricts translational and rotational diffusion from six to two dimensions, and the binding encounter frequency is increased 150-fold; since k_{cat} is nearly unaffected, the catalytic module is disengaged from membrane binding (Fig. 4).

The high affinity of fIXaβ for fVIIIa (58, 59, 61) implies an extended interaction surface between the two factors, provided especially by the EGF-2 and catalytic modules of fIXaβ (47–50). We suggest that the arched fIXaβ molecule lies across a substructure of fVIIIa, with the fIXaβ surface described above providing most of the contacts (see Fig. 4). Since fVIIIa does not influence the activity of fIXaβ toward chromogenic substrates or chloromethyl ketones (10–14), formation of the fIXaβ–fVIIIa binary complex would not complete active site formation and rigidification at the hypothetically collapsed S1 site, even in the presence of phospholipid. Instead, we suggest that binding of spatially similar but less rigid fX to the opposite side of fVIIIa could force the fX cleavage sites close to the substrate binding site of fIXaβ and provide the energy for active site rigidification (see Fig. 4). This could explain why, in the absence of phospholipid, fVIIIa binding enhances k_{cat} 300-fold but minimally affects the K_m value (63–65), since the energy of cofactor binding is diverted to active site formation. Addition of phospholipid, which reduces the degrees of free-

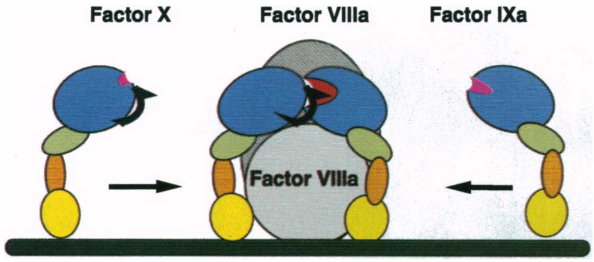

FIG. 4. Schematic drawing of intrinsic Xase complex formation. In the absence of fVIIIa, the specificity pocket of fIXa is mobile and incompletely formed. The bent fIXaβ molecule could arch across a substructure of fVIIIa [represented as a compact membrane-bound molecule of dimensions roughly similar to those recently derived for fVa from electron microscopy (60)] and simultaneously interact with the elongated fVIIIa substructure through residues on the left side (with respect to Fig. 1). fX, of a similar overall shape, arches across the fVIIIa substructure from the opposite side; interaction forces the activation cleavage site Arg-194–Ile-195 into the fIXaβ active site, opening the S1 specificity pocket and enabling activation cleavage.

dom by preorienting the factors for complexation, leads to a 100-fold reduction in K_m (to 60 nM; i.e., far beyond plasma concentration) and a further 10-fold enhancement in k_{cat} [8 sec^{-1} (58, 59)].

The structure of fIXaβ presented here allows a more reliable assessment of the structural and functional importance of specific residues, in particular those susceptible to deleterious mutants (36–38), and thus an understanding of the molecular mechanisms underlying hemophilia B. The Xase model shown in Fig. 4 is a starting point in understanding the millionfold enhancement in the catalytic efficiency of fIXaβ upon formation of the intrinsic Xase complex; aspects of this model might be transferable to related structures such as the prothrombinase complex. It provides a framework for localizing the interaction sites involved in Xase function, making testable predictions of sites suitable for mutagenesis experiments.

This paper is dedicated to Prof. Dr. Hans Frik on the occasion of his 60th birthday. We thank Drs. J. Stenflo and I. D. Campbell for providing their NMR structures before release, Dr. E. J. Duffy for assistance in purification of fIXaβ, and Drs. R. A. Engh and M. T. Stubbs for invaluable discussions. The financial support of the SFB207 and of the Fonds der Chemischen Industrie is gratefully acknowledged.

1. Kurachi, K., Kurachi, S., Furukawa, M. & Yao, S.-N. (1993) *Blood Coagulation Fibrinolysis* **4**, 953–974.
2. Limentani, S. A. & Furie, B. (1995) in *Haematology: Basic Principles and Practice*, eds. Hoffman, R., Bentz, E. G., Shattil, S. J., Furie, B., Cohen, H. G. & Silverstein, L. (Churchill Livingstone, New York), pp. 1664–1678.
3. Rainer, A. P. & Davie, E. W. (1994) in *Haemostasis and Thrombosis* (Churchill Livingstone, New York), pp. 309–331.
4. Lollar, P., Parker, C. G., Kajenski, P. J., Litwiller, R. D. & Fass, D. N. (1987) *Biochemistry* **26**, 7627–7636.
5. Sarkar, G., Koeberl, D. D. & Sommer, S. S. (1990) *Genomics* **6**, 133–143.
6. Sarkar, G., Turner, R. T. & Bolander, M. E. (1993) *PCR Methods Appl.* **2**, 318–322.
7. Fujikawa, K., Coan, M. H., Legaz, M. E. & Davie, E. W. (1974) *Biochemistry* **13**, 5290–5299.
8. Kurachi, K., Davie, E. W. (1982) *Proc. Natl. Acad. Sci. USA* **79**, 6461–6464.
9. Yoshitake, S., Schach, B. G., Foster, D. C., Davie, E. W. & Kurachi, K. (1985) *Biochemistry* **24**, 3736–3750.
10. Byrne, R., Link, R. P. & Castellino, F. J. (1980) *J. Biol. Chem.* **255**, 5336–5341.
11. McRae, B. J., Kurachi, K., Heimark, R. L., Fujikawa, K., Davie, E. W. & Powers, J. C. (1981) *Biochemistry* **20**, 7196–7206.
12. Castillo, M. J., Kurachi, K., Nishino, N., Okkubo, F. & Powers, J. C. (1983) *Biochemistry* **22**, 1021–1029.
13. Butenas, S., Orfeo, T., Lawson, J. H. & Mann, K. G. (1992) *Biochemistry* **31**, 5399–5411.
14. Kam, C. M., Kerrigan, J. E., Plaskon, R. R., Duffy, E. J., Lollar, P., Suddath, F. L. & Powers, J. C. (1994) *J. Med. Chem.* **37**, 1298–1306.
15. van Dieijen, G., Tans, G., Rosing, J. & Hemker, H. C. (1981) *J. Biol. Chem.* **256**, 3433–3442.
16. Bode, W., Mayr, I., Baumann, U., Huber, R., Stone, S. R. & Hofsteenge, J. (1989) *EMBO J.* **8**, 3467–3475.
17. Bode, W., Turk, D. & Karshikov, A. (1992) *Protein Sci.* **1**, 426–471.
18. Rydel, T. J., Ravichandran, K. G., Tulinsky, A., Bode, W., Huber, R., Roitsch, C. & Fenton, J. W. (1990) *Science* **249**, 277–280.
19. Arni, R. K., Padmanabhan, K., Padmanabhan, K. P., Wu, T. P. & Tulinsky, A. (1993) *Biochemistry* **32**, 4727–4737.
20. Seshadri, T. P., Tulinsky, A., Skrzypczak-Jankun, E. & Park, C. H. (1991) *J. Mol. Biol.* **220**, 481–494.
21. Soriano-Garcia, M., Padmanabhan, K., de Vos, A. M. & Tulinsky, A. (1992) *Biochemistry* **31**, 2554–2566.
22. Padmanabhan, K., Padmanabhan, K. P., Tulinsky, A., Park, C. H., Bode, W., Huber, R., Blankenship, D. T., Cardin, A. D. & Kisiel, W. (1993) *J. Mol. Biol.* **232**, 947–966.
23. Baron, M., Norman, D. G., Harvey, T. S., Handford, P. A., Mayhew, M., Tse, A. G., Brownlee, G. G. & Campbell, I. D. (1992) *Protein Sci.* **1**, 81–90.
24. Selander-Sunnerhagen, M., Ullner, M., Persson, E., Teleman, O., Stenflo, J. & Drakenberg, T. (1992) *J. Biol. Chem.* **267**, 19642–19649.
25. Sunnerhagen, M., Forsen, S., Hoffren, A. M., Drakenberg, T., Teleman, O. & Stenflo, J. (1995) *Nature Struct. Biol.* **2**, 504–509.
26. Freedman, S. J., Furie, B. C., Furie, B. & Baleja, J. D. (1995) *J. Biol. Chem.* **270**, 7980–7989.
27. Lollar, P., Knutson, G. J. & Fass, D. N. (1984) *Blood* **63**, 1303–1308.
28. Lollar, P. & Fass, D. N. (1984) *Arch. Biochem. Biophys.* **233**, 438–446.
29. Collaborative Computational Project Number 4 (1994) *Acta Crystallogr.* **D50**, 760–763.
30. Brünger, A. T. (1993) X-PLOR (Yale Univ. Press, New Haven, CT), Version 3.1.
31. Turk, D. (1992) Ph.D. thesis (Technische Universität, Munich).
32. Navaza, J. (1994) *Acta Crystallogr.* **A50**, 157–163.
33. Evans, S. V. (1990) *J. Mol. Graphics* **11**, 134.
34. Nicholls, A. & Honig, B. (1992) GRASP (Columbia Univ., New York), Version 1.1.
35. Hamaguchi, N., Roberts, H. & Stafford, D. W. (1993) *Biochemistry* **32**, 6324–6329.
36. Bottema, C. D., Ketterling, R. P., Ii, S., Yoon, H. S., Phillips, J. A., III, & Sommer, S. S. (1991) *Am. J. Hum. Genet.* **49**, 820–838.
37. Roberts, H. R. (1993) *Thromb. Haemostasis* **70**, 1–9.
38. Gianelli, F., Green, P. M., Sommer, S. S., Lillicrap, D. P., Ludwig, M., Schwaab, R., Reitsma, P. H., Goossens, M. & Brownlee, G. G. (1994) *Nucleic Acids Res.* **22**, 3534–3546.
39. Huber, R. & Bode, W. (1978) *Acc. Chem. Res.* **11**, 114–122.
40. Bode, W., Schwager, P. & Huber, R. (1978) *J. Mol. Biol.* **118**, 99–112.
41. Bode, W. (1979) *J. Mol. Biol.* **127**, 357–374.
42. Wang, D., Bode, W. & Huber, R. (1985) *J. Mol. Biol.* **185**, 595–624.
43. Vijayalakschmi, J., Padmanabhan, K. P., Mann, K. G. & Tulinsky, A. (1994) *Protein Sci.* **3**, 2254–2271.
44. Astermark, J., Bjork, I., Ohlin, A. K. & Stenflo, J. (1991) *J. Biol. Chem.* **266**, 2430–2437.
45. Wolberg, A. S., Cheung, W. F., Stafford, D. W. & Hamaguchi, N. (1993) *Thromb. Haemostasis* **69**, 614 (abstr.).
46. Jacobs, M., Freedman, S. J., Furie, B. C. & Furie, B. (1994) *J. Biol. Chem.* **269**, 25494–25501.
47. Medved, L. V., Vysotchin, A. & Ingham, K. C. (1994) *Biochemistry* **33**, 478–485.
48. Cheung, W. F., Hamaguchi, N., Smith, K. J. & Stafford, D. W. (1992) *J. Biol. Chem.* **267**, 20529–20531.
49. Mutucumarana, V. P., Duffy, E. J., Lollar, P. & Johnson, A. E. (1992) *J. Biol. Chem.* **267**, 17012–17021.
50. Astermark, J., Hogg, P. J., Bjork, I. & Stenflo, J. (1992) *J. Biol. Chem.* **267**, 3249–3256.
51. Ahmad, S. S., Rawala-Sheikh, R., Cheung, W.-F., Stafford, D. W. & Walsh, P. N. (1992) *J. Biol. Chem.* **267**, 8571–8576.
52. Bajaj, S. J., Rapaport, S. I. & Maki, S. L. (1985) *J. Biol. Chem.* **260**, 11574–11580.
53. Lin, S. W., Smith, K. J., Welsh, D. & Stafford, D. W. (1990) *J. Biol. Chem.* **265**, 144–150.
54. Hertzberg, M. S., Ben-Tal, O., Furie, B. & Furie, B. C. (1992) *J. Biol. Chem.* **267**, 14759–14766.
55. Hughes, P. E., Morgan, G., Rooney, E. K., Brownee, G. G. & Handfood, P. (1993) *J. Biol. Chem.* **268**, 17727–17733.
56. Hase, S., Kawabata, S., Nishimura, H., Takeya, H., Sueyoshi, T., Miyata, T., Iwanaga, S., Takao, T., Shimonishi, Y. & Ikenaka, T. (1988) *J. Biochem. (Tokyo)* **104**, 867–868.
57. Kisiel, W., Smith, K. J. & McMullen, B. A. (1985) *Blood* **66**, 1302–1308.
58. Nishimura, H., Takoo, T., Hase, S., Shimonishi, Y. & Iwanaga, S. (1992) *J. Biol. Chem.* **267**, 17520–17525.
59. Nishimura, H., Takeya, H., Miyata, T., Suehiro, K., Okamura, T., Niho, Y. & Iwanaga, S. (1993) *J. Biol. Chem.* **268**, 24041–24046.
60. Stoylova, S., Mann, K. G. & Brisson, A. (1994) *FEBS Lett.* **351**, 330–334.
61. Duffy, E. J., Parker, E. T., Mutucumarana, V. P., Johnson, A. E. & Lollar, P. (1992) *J. Biol. Chem.* **267**, 17006–17011.
62. Wacey, A. I., Krawczak, M., Kakkar, V. V. & Cooper, D. N. (1994) *Hum. Genet.* **94**, 594–608.
63. Duffy, E. J. & Lollar, P. (1992) *J. Biol. Chem.* **267**, 7821–7827.
64. Barrow, R. T., Parker, E. T., Krishnaswamy, S. & Lollar, P. (1994) *J. Biol. Chem.* **269**, 26796–26800.
65. van Dieijen, G., van Rijn, J. L. M. L., Govers-Riemslag, J. W. P., Hemker, H. C. & Rosing, J. (1985) *Thromb. Haemostasis* **53**, 396–400.